AKADÉMIAI KIADÓ

UNIVERSITY of DEBRECEN

International Review of Applied Sciences and Engineering

15 (2024) 1, 29–43

DOI:
10.1556/1848.2023.00635

ORIGINAL RESEARCH PAPER

Development of a 2-dimensional thermal calculation method to estimate silicone oil's temperature distribution in viscous torsional vibration dampers

M. Venczel[1*], Á. Veress[1,2] and Z. Peredy[3]

[1] Department of Aeronautics and Naval Architecture, Faculty of Transportation Engineering and Vehicle Engineering, Budapest University of Technology and Economics, Műegyetem rkp. 3, H-1111, Budapest, Hungary

[2] Knorr-Bremse R&D Center Budapest, Engineering Calculations, Major utca 69, H-1119, Budapest, Hungary

[3] Engineering Institute, Edutus University, Stúdium tér 1, H-2800, Tatabánya, Hungary

Received: January 27, 2023 • Accepted: April 4, 2023
Published online: May 22, 2023

ABSTRACT

High-performance internal combustion engines are subject to severe torsional vibrations which result from uneven gas and inertial loads. Fatigue damage occurs if the frequency of these undesired oscillations matches the resonance frequency of the crankshaft and the driven engine elements. This phenomenon can be avoided by the application of visco-dampers whose working fluid is high-viscosity silicone oil. Since silicone oil is exposed to a significant amount of heat load during operation, it is essential to calculate the temperature distribution in a relatively easy, quick, and cost-efficient way for lifetime estimation purposes. The aim of this article is to develop a reliable, fast, and accurate finite difference-based numerical method for steady-state thermal calculations for arbitrary damper sections. The developed MATLAB code calculates the temperature field of the damping fluid together with all components in a radial cross-section at given operational conditions. The accuracy of the developed thermal calculation method has been tested in a 3-dimensional – 2-dimensional two-step verification process by finite element and finite volume-based advanced engineering software in ANSYS environment. Furthermore, the original Iwamoto equation available in the literature has been updated to provide more accurate surface temperature results based on the simulations' outcome gained by the finite volume method.

KEYWORDS

finite difference method, heat transfer, CFD, MATLAB, thermal analysis, silicone oil, Iwamoto-equation, torsional vibration damper

1. INTRODUCTION

Vibration is considered a periodic mechanical event when oscillations arise at an equilibrium point and is considered frequently an unpleasant phenomenon because it consumes energy and generates unwelcome sound, friction, abrasion, deformation, rising temperature or stress, and fatigue. Fatigue damage can occur in case the oscillation frequency is corresponding with the eigenfrequency of the crankshaft and driven components [1].

As an internal combustion engine releases thermal energy by burning fuel in the piston cylinders, the connecting rods on the crankshaft transform this thermal energy into mechanical load (torque). Unfavourable oscillations on the shaft and significant mechanical tension in the drivetrain are brought on by the repeated occurrence of transient angular

*Corresponding author.
E-mail: mvenczel@vrht.bme.hu

acceleration (specified by the ignition and injection sequence). These oscillations tend to reduce the power of the engine and are responsible for noise and abrasion.

In order to prevent the fatigue damage, to extend the service life of the engine and to reduce the generated noise and vibration amplitude of the crankshaft, camshaft, and fuel pump, a torsional vibration damper (TVD) can be integrated into the flywheel or assembled on the crankshaft. Today, TVDs are widely utilized in heavy-duty piston engines in the automobile sector (race cars, commercial vehicles, ships, and airplanes), as well as in the military, architectural, agricultural, and mining areas.

One type of these damping devices is the viscous torsional vibration damper (shortly visco-damper) whose working fluid is a high-viscosity silicone oil. As presented in Fig. 1, one of the simplest devices in damping technology is the visco-dampers with low maintenance cost because they are built up from an inertia-ring that is free to move and a closed annular space (housing) around the inertia-ring. A thin coating of silicone fluid surrounds the inertia-ring, which is supported by a polymer slide bearing.

This is how the damping effect of the visco-damper works: when the crankshaft rotates smoothly without any vibration, the inertia-ring travels in synchrony with the housing without slipping. The housing and the inertia-ring start to move relative to one another as soon as a slight torsional oscillation appears, and the oil experiences circumferential shear stress. This shear stress computed on the friction surfaces between the housing-cover and the inertia-ring is added up to provide the damping effect. Since silicone oil is considered as a non-Newtonian fluid, it reacts differently to external impact than other typical (Newtonian) fluids. Because of this, the relative velocity difference between the housing and the inertia-ring affects the oil's viscosity and, in turn, its damping properties: higher velocity differences between the components next to the silicone oil cause lower viscosity.

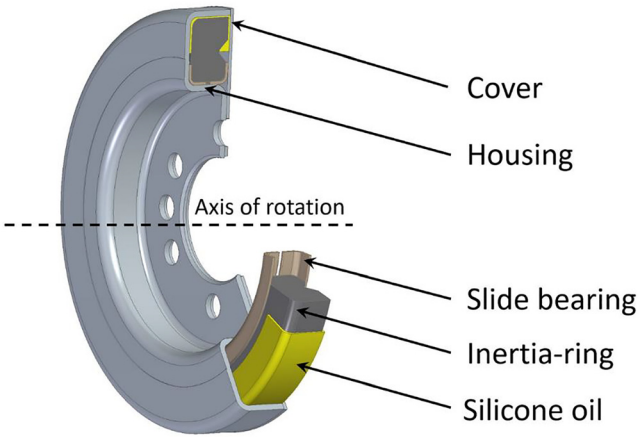

Fig. 1. Structure of a visco-damper in section view (own source)

When a visco-damper is in operation, the damping medium is subjected to a significant amount of thermal load that results from the friction and shear of the oil layers as well as from the heat originating from the engine. Since there is no proper and safe thermal measurement technology and methodology in the course of the TVD in operation, it is inevitable to be able to estimate the silicone oil's temperature distribution during operation to minimize oil degradation level, significantly prolong the lifetime of TVD and the service life of the internal combustion engine [2] by identifying and analyzing the life-span influencing factors of the oil. Only numerical calculations can be potential solutions for giving answers to thermal, mechanical, and lifetime questions in a relatively easy, quick, and cost-efficient way.

Several studies deal with the calculation of operating temperature and the internal thermal condition of visco-dampers. In 2012, Wang et al. [3] introduced a coupling calculation technique based on the heat balance for silicone oils and dampers with high accuracy in engineering applications. In this calculation method, the crankshaft and the damper are simplified to a model of torsion with a single shaft that has the same inherent frequency and oscillation energy.

In 2015, Forberger [4] used three material models (Maxwell, Upperconvected Maxwell, and Oldroyd-B) to calculate the dissipated power in a visco-damper. The presented method with the three material models is compared in a transient, non-isothermal, finite element calculation and the result is used to check with measurements.

In 2021, Homik et al. [5] proposed a model for TVDs using thermo-hydrodynamics that can effectively support the process of matching a damper for a given drive unit. The developed model is used to determine the correct operating surface temperature range of the damper's housing in steady-state operation. The correctness of the developed thermo-hydrodynamic model was verified both by a numerical simulation and by test bench measurements on a six-cylinder diesel engine equipped with a factory TVD.

Based on the studies of [3–5], different analysis approaches and complex calculation models have been introduced for visco-dampers so far, however, none of the above-mentioned studies provides a calculation method to reveal the temperature distribution in the whole structure of the visco-damper with special regard for the temperature distribution of the silicone oil. Thus, the aim of this article is to develop a fast, reliable, accurate and verificated 2-dimensional numerical method for thermal calculations in a given radial damper section. The developed MATLAB code is suitable to calculate the temperature field of the damping fluid and the whole damper structure under given operational conditions for lifetime estimation purposes. Expectation towards the core calculation method is to be extended, as a design tool of the R&D activities, for being capable of calculating arbitrary damper geometries in the future. Table 1 briefly summarizes the main factors which the developed model should be able to handle.

Table 1. Requirements for the developed 2-dimensional thermal calculation method (own source)

Name of the factor	Main characteristics of the factor
Domains with different material properties	• structural steel • silicone oil • air
Basic thermal phenomena	• heat convection • heat conduction • heat transfer through ideal contacts • heat generation • perfect insulation
Assumptions and simplifications in the developed model	• silicone oil and air-gap are treated as solid domains • heat radiation is negligible • the effect of cooling fins mounted on the housing is out of focus • the heating effect of engine is out of focus • generated heat and convected heat are the function of radius • calculation is performed for a unit time in steady state condition
Additional requirements	• adjustable geometry • adjustable filling level for silicone oil • adjustable numerical mesh • prompt calculation and evaluation • visualisation of the numerical results

2. DEVELOPMENT OF A VISCO-DAMPER SPECIFIC THERMAL CALCULATION METHOD

2.1. Finite difference method (FDM)

The explanation of the physical principles governing space- and time-dependent issues is typically represented in terms of partial differential equations, which are frequently difficult to solve analytically across arbitrary geometries or cannot be solved at all. Instead, a rough approximation of the equations based on various discretization methods can be created. The finite difference method (FDM) is the very first and general discretization technique for many kinds of engineering problems. The fundamental idea behind this method is the local Taylor expansion used to rough approximation of the partial differential equations. The partial differential equations are discretized through square network of lines determining a very regular, fine and structured mesh. This means the primary drawback of this numerical approach when dealing with complex geometry [6, 7]. FDM has been used for this work considering its advantages: a) quickest method for solving simple differential equations; b) works well with simple geometries; c) most intuitive to understand and easy to learn; d) easy to implement in computer programs.

Let us introduce two different definitions for the first-order derivative in the x direction based on Fig. 2. The forward Euler approximation can be expressed by Eq. (1) while the backward Euler approximation is presented by Eq. (2). These equations basically say that the slope of a curve $\left(\frac{\partial u}{\partial x}\right)$ at a certain point $(u(x_i))$ can be approximated by the slope calculated from two points of that curve in Δx distance, apart from each other (as shown in Fig. 2.). As Δx approaches to zero, the difference between the calculated and the real value of the derivative becomes smaller. By applying a Taylor expansion to the term $u(x+\Delta x)$ and $u(x-\Delta x)$ until the first-order term, one can arrive at a comparable derivative representation [7, 8].

$$\frac{\partial u}{\partial x} = \lim_{\Delta x \to 0} \frac{u(x+\Delta x) - u(x)}{\Delta x} \tag{1}$$

$$\frac{\partial u}{\partial x} = \lim_{\Delta x \to 0} \frac{u(x) - u(x-\Delta x)}{\Delta x} \tag{2}$$

The general formula for Taylor series expansion can be expressed in Eq. (3). Applying Eq. (3) for Forward Taylor will gain Eq. (4) while applying Eq. (3) for Backward Taylor will gain Eq. (5).

$$u(x) = \sum_{n=0}^{\infty} \frac{(x-x_i)^n}{n!} \left(\frac{\partial^n u}{\partial x^n}\right)_i \tag{3}$$

$$\begin{aligned} u(x+\Delta x) &= u_{i+1} \\ &= u_i + \Delta x \left(\frac{\partial u}{\partial x}\right)_i + \frac{(\Delta x)^2}{2!} \left(\frac{\partial^2 u}{\partial x^2}\right)_i \\ &\quad + \frac{(\Delta x)^3}{3!} \left(\frac{\partial^3 u}{\partial x^3}\right)_i + \ldots \end{aligned} \tag{4}$$

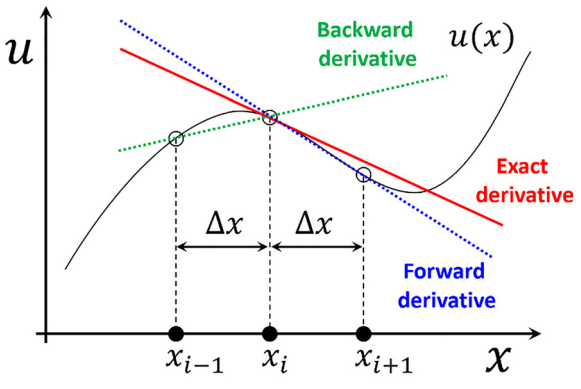

Fig. 2. Approximating the slope of a curve in a point (own source)

$$u(x-\Delta x) = u_{i-1} = u_i - \Delta x\left(\frac{\partial u}{\partial x}\right)_i + \frac{(\Delta x)^2}{2!}\left(\frac{\partial^2 u}{\partial x^2}\right)_i - \frac{(\Delta x)^3}{3!}\left(\frac{\partial^3 u}{\partial x^3}\right)_i + \dots \quad (5)$$

The forward difference expressed by Eq. (6) can be derived by the rearrangement of Eq. (4) while the backward difference presented by Eq. (7) will be gained from Eq. (5) with similar consideration.

$$\left(\frac{\partial u}{\partial x}\right)_i = \frac{u_{i+1}-u_i}{\Delta x} - \frac{\Delta x}{2!}\left(\frac{\partial^2 u}{\partial x^2}\right)_i - \frac{(\Delta x)^2}{3!}\left(\frac{\partial^3 u}{\partial x^3}\right)_i - \dots = \frac{u_{i+1}-u_i}{\Delta x} + O(\Delta x) \quad (6)$$

$$\left(\frac{\partial u}{\partial x}\right)_i = \frac{u_i-u_{i-1}}{\Delta x} + \frac{\Delta x}{2!}\left(\frac{\partial^2 u}{\partial x^2}\right)_i - \frac{(\Delta x)^2}{3!}\left(\frac{\partial^3 u}{\partial x^3}\right)_i + \dots = \frac{u_i-u_{i-1}}{\Delta x} + O(\Delta x) \quad (7)$$

Where $O(\Delta x)$ is the error committed in terminating the series and is referred to as truncation error. It can be negligible in the further calculations.

2.2. Geometry equivalence theory

Considering the cylindrical symmetry of the TVDs, it is sufficient to perform thermal calculations only in a well-defined radial cross-section of the geometry. Providing the fact that the homogeneous and isotropic material properties, boundary conditions and the temperature distribution are the same in each radial section of the damper. In order to make the thermal calculations and programming easier, some simplifications (listed below) have been done on the damper geometry. Figure 3 presents the simplified geometry.

The applied geometry simplifications are as follows:

- cover and house are merged together and a symmetric, uniform toroidal case has been created;
- case, oil and inertia-ring have common rounding centre in each corner;
- the charging chambers in the inertia-ring has been removed;
- the slide bearings have been removed and replaced with air since the material of slide bearings may change per applications, but the thermal conductivity of air is always the same and its value is lower by four orders of magnitude compared to the plastics;
- the thickness of gap-size is uniform along the inertia-ring periphery.

As finite difference method has been applied for this work, it is important to use a uniform numerical grid for the calculations with the same cell-size both in vertical and horizontal directions. The numerical grid is built up from uniform squares which are not suitable to overlap properly a real damper cross-sectional area with roundings and curvatures. Because of this fact, a geometrical transformation must have been applied to turn the simplified damper cross-section into a rectangular area. The equivalence considerations of this transformation are discussed below.

In Fig. 4., the left side presents the subdivision lines and the subdivided cross-section elements of the simplified damper geometry with sequence numbers. Each line must be perpendicular to the oil band and to the surface of the case. As the geometry is cut along the cut-in line at the first element (marked by a black line in Fig. 4.) and "opened-up" according to the arrows, a 2-dimensional equivalent geometry will be obtained (see Fig. 5c). It is clearly seen in Fig. 5b, that the thickness of case and oil film remained unchanged, however, the thickness of inertia-ring became ambiguous. Thus, an equivalent inertia-ring thickness must be calculated that provides the same area compared to the simplified closed geometry (marked with green colour in the right side of Fig. 4 and in Fig. 5a).

The length of the equivalent geometry is equal to the length of the damper gap in the original geometry. The equivalent inertia-ring thickness can be obtained from a simple area calculation by Eq. (8).

$$h_{eq} = \frac{A_{ring}}{L} \quad (8)$$

Where h_{eq} is the equivalent inertia-ring thickness [m], A_{ring} is the area of inertia-ring of closed geometry [m^2] and L is the length of damper gap in the original damper geometry [m].

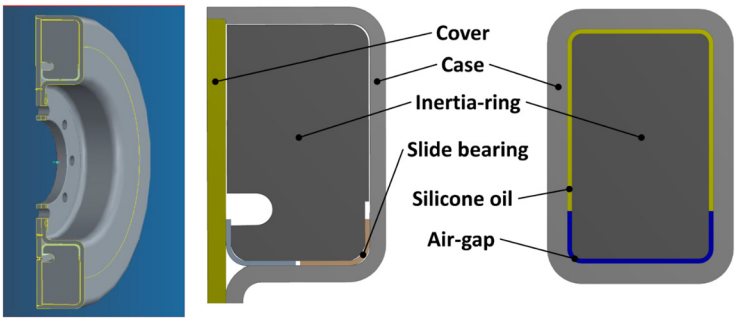

Fig. 3. CAD model of a real viscous TVD (left), components of the TVD (middle), simplified 2-dimensional thermal model (right) (own source)

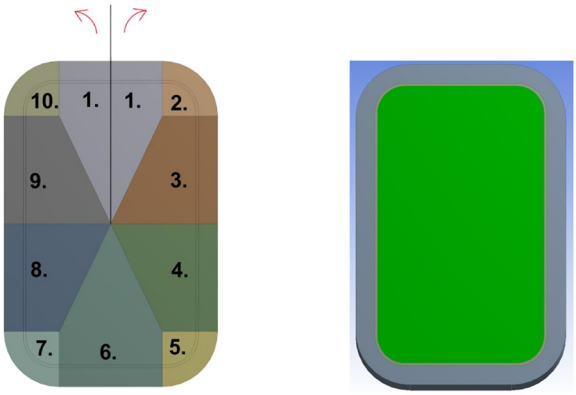

Fig. 4. Subdivision (left side) and ring area (right side) of the simplified geometry (own source)

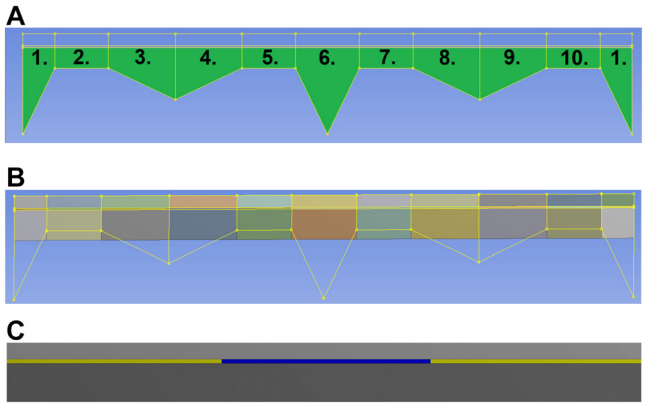

Fig. 5. a. Opening-up the subdivided damper cross-section with ambiguous thickness of the inertia-ring; b. The equivalent inertia-ring thickness; c. The 2-dimensional equivalent damper geometry (own source)

2.3. Visco-damper specific heat-transfer calculations

Focusing on the 2-dimensional equivalent damper geometry, the developed thermal calculation method must involve typical thermal phenomena collected in the second row of Table 1. Next step was finding proper formula for each mentioned thermal phenomenon to apply them in the nodes of the finite different mesh. Only the initial and final form of the derived formulas are presented and put into the damper thermal calculation code.

2.3.1. Heat conduction. Figure 6 shows a detailed view of a uniform finite difference mesh where the grid spacing both in x and y direction is equal. The temperature in node $N(i,j)$ can be obtained with the help of the surrounding nodal temperature values.

The general differential equation of heat conduction can be described by Eq. (9) [8].

$$\frac{1}{\boldsymbol{a}}\frac{\partial T}{\partial \boldsymbol{t}} = \nabla^2 T + \frac{\dot{q}_v}{\lambda} \tag{9}$$

Where a is the temperature conductivity factor or thermal diffusivity $\left[\frac{m^2}{s}\right]$, T is the temperature variable $[K]$, t is the time $[s]$, $\dot{q}_v$ is the volume heat source $\left[\frac{W}{m^3}\right]$, and λ is the thermal conductivity $\left[\frac{W}{m\,K}\right]$.

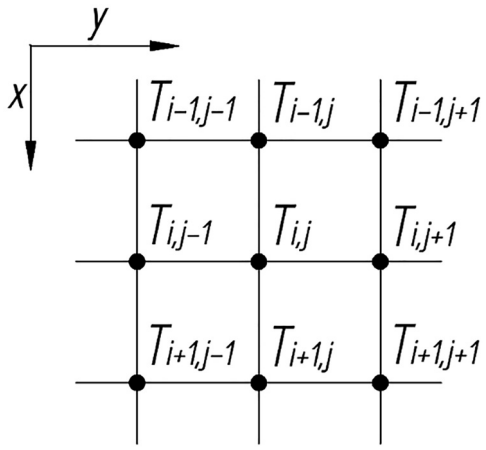

Fig. 6. Detail of a uniform FDM mesh (own source)

In the case of steady state condition without heat generation in 2-dimensional space the above equation is simplified into the Laplace's equation presented by Eq. (10) [8].

$$0 = \nabla^2 T = \frac{\partial^2 T}{\partial x^2} + \frac{\partial^2 T}{\partial y^2} \tag{10}$$

After expanding the partial derivatives into Taylor series and applying forward and backward differences twice, the $N(i,j)$ final nodal temperature formula of heat conduction for finite difference method will be given by Eq. (11).

$$T_{i+1,j} + T_{i,j+1} - 4T_{i,j} + T_{i-1,j} + T_{i,j-1} = 0 \tag{11}$$

2.3.2. Heat generation. Although there are several sophisticated models for thermodynamic approach of friction, wear and temperature rise in tribology [9, 10], damping power (or dissipated heat) has been applied in this work as a heat load on the oil, since this type of quantity is the typical input in the thermal calculation of visco-dampers in the industry.

The volume heat source is considered as the damping power divided by the oil volume, where the amount of heat, generated in a given point of the oil-gap, is the function of radius (radial distance measured from the axis of rotation). A simplified formula can be used to estimate the radius dependent heat source value in each point of the discretized oil domain by Eq. (12).

$$\dot{q}_v(r) = \frac{\dot{Q}_{damp}(r)}{V_{oil}(r)} \tag{12}$$

Where $\dot{q}_v(r)$ is the radius-dependent volume heat source $\left[\frac{W}{m^3}\right]$, $\dot{Q}_{damp}(r)$ is the radius-dependent damping power $[W]$, $V_{oil}(r)$ is the radius-dependent volume of oil $[m^3]$ and r is the radial distance from the axis of rotation [m].

In oil nodes, where heat generation occurs, a heat source term has been added to the Laplace's equation, forming the Poisson's equation as presented by Eq. (13) [8].

$$0 = \nabla^2 T + \frac{\dot{q}_v}{\lambda} = \frac{\partial^2 T}{\partial x^2} + \frac{\partial^2 T}{\partial y^2} + \frac{\dot{q}_v}{\lambda} \tag{13}$$

After similar derivations and rearrangements, the $N(i,j)$ final nodal temperature formula with heat generation for finite difference method is gained by Eq. (14).

$$T_{i+1,j} + T_{i,j+1} - 4T_{i,j} + T_{i-1,j} + T_{i,j-1} = -\frac{\dot{q}_v \delta^2}{\lambda} \tag{14}$$

Where $\delta = \Delta x = \Delta y$ is the grid spacing [m].

2.3.3. Heat convection. Heat is transferred via heat conduction in the material from higher temperature zones to the lower one. As the outside bounding surface is reached (see blue (or lighter) nodes of Fig. 7), heat dissipates to the ambient in form of heat convection. The conducted and convected amount of heat, perpendicularly to the surface, must be equal. The same equation can be written for each surface nodes.

The differential form of Fourier's Law of thermal conduction [8] is described by Eq. (15).

$$\dot{q} = -\lambda \nabla T \tag{15}$$

Where $\dot{q}$ is the heat flux $\left[\frac{W}{m^2}\right]$, λ is the thermal conductivity $\left[\frac{W}{m\,K}\right]$, ∇ is the Nabla operator and T is the temperature variable $[K]$.

Only in x direction the formula is given by Eq. (16).

$$\dot{q}_x = -\lambda \frac{\partial T}{\partial x} \tag{16}$$

As there is no nodal information above the surface (ambient is not modelled), backward difference has been applied for the partial derivatives. It has been expanded into a Taylor series reduced to the second-order terms for second-order accuracy. Thus, the heat flux equation only in x direction is given by Eq. (17).

$$\frac{-\lambda}{2\Delta x}\left(4T_{i+1,j} - 3T_{i,j} - T_{i+2,j}\right) = -\alpha\left(T_{i,j} - T_{ambient}\right) \tag{17}$$

Where α is the heat transfer coefficient $\left[\frac{W}{m^2\,K}\right]$ and $T_{ambient}$ is the ambient temperature [K].

After some rearrangements the $N(i,j)$ final nodal temperature formula of heat convection for finite difference method can be obtained only in x direction by Eq. (18).

$$T_{i,j}\left(-3 - \frac{2\alpha\Delta x}{\lambda}\right) + 4T_{i+1,j} - T_{i+2,j} = -\frac{2\alpha\Delta x}{\lambda} T_{ambient} \tag{18}$$

As far as visco-damper in rotation is concerned, the heat transfer coefficient on the outer surface of the case is the function of peripheral speed and an empirical formula has been used to determine the accurate heat transfer coefficient of each node of the case surface expressed by Eq. (19) [3].

$$\alpha = 7.8 \cdot (0.75 \cdot \omega \cdot r)^{0.75} \tag{19}$$

Where α is the heat transfer coefficient $\left[\frac{W}{m^2\,K}\right]$, ω is the angular velocity of the damper housing $\left[\frac{rad}{s}\right]$ and r is the radial distance from the axis of rotation [m].

2.3.4. Interface connection. At the boundary of two adjacent domains with different materials an interface has been defined which is considered a type-four ideal contact (see pink (or lighter) nodes in Fig. 8). It assumes the fact that the roughness of the surfaces is negligible and the heat flux, perpendicular to the interface, is constant. In the case of Poisson's equations, where different materials are taken into account, the contact temperature in the interface can be determined from the heat conduction equation only in y direction by Eq. (20).

$$\frac{-\lambda_1}{\Delta y}\left(T_{i,j} - T_{i,j-1}\right) = \frac{-\lambda_2}{\Delta y}\left(T_{i,j+1} - T_{i,j}\right) \tag{20}$$

After some rearrangements, the $N(i,j)$ final nodal temperature formula of interface connection for finite difference method only in y direction is gained by Eq. (21).

$$T_{i,j} = \frac{\lambda_1 T_{i,j-1} + \lambda_2 T_{i,j+1}}{\lambda_1 + \lambda_2} \tag{21}$$

2.3.5. Identical boundary condition. As the simplified model is cut-in and opened-up, identical condition must be applied along the cut-in line (see green (or lighter) nodes in Fig. 9).

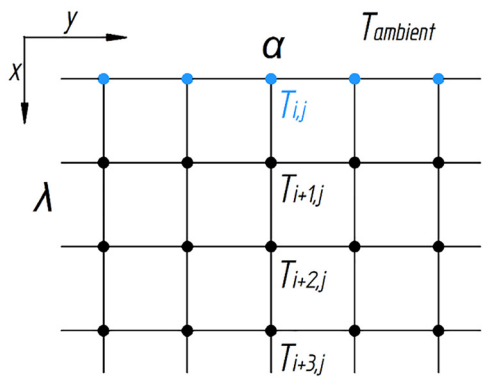

Fig. 7. Nodes with heat conduction and heat convection in the FDM mesh (own source)

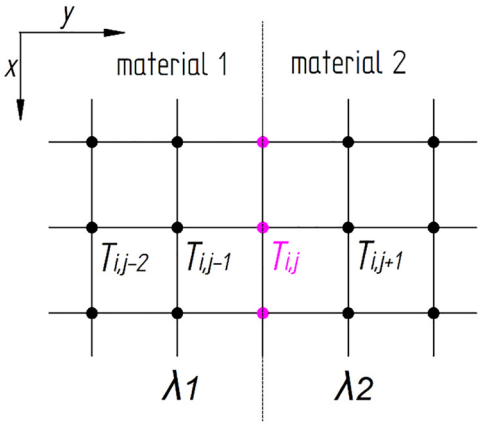

Fig. 8. Type-four ideal contact in FDM mesh (own source)

This type of boundary condition provides the fact that the nodes along the vertical side-edges of the equivalent geometry belong together and represent a common node in spite of the nodal duplication. These nodes belong to the same material in pairs, thus, the $N(i,j)$ final nodal temperature formula of interface connection only in y direction will gain a simpler form presented by Eq. (22).

Since $\lambda_1 = \lambda_2 = \lambda$

$$T_{i,j} = \frac{\lambda_1 T_{i,j-1} + \lambda_2 T_{i,j+1}}{\lambda_1 + \lambda_2} = \frac{\lambda\left(T_{i,j-1} + T_{i,j+1}\right)}{2\lambda} = \frac{T_{i,j-1} + T_{i,j+1}}{2} \tag{22}$$

2.3.6. Perfect insulation. There is no information about the temperature of inertia-ring midpoint, thus it is considered to be an isolated point and a perfect insulation boundary condition has been applied onto the last row nodes (see orange (or lighter) nodes in Fig. 10) in the damper 2-dimensional equivalent geometry. Thermal insulation provides an isolated region in which thermal conduction and the heat flow rate, perpendicular to the wall, is reduced to zero. Thus, the $N(i,j)$ final nodal temperature formula for insulation for finite difference method only in x direction is presented by Eq. (23).

$$T_{i,j} = T_{i-1,j} \tag{23}$$

2.4. Setting up an example calculation in MATLAB environment

According to the previously discussed part, the geometry, the meshing, and the discretized form of the governing equations are available as a basic for the FDM analysis. Figure 11 briefly summarizes the necessary system of equations and the main steps for solving the damper thermal problem in MATLAB environment.

The code script of the developed damper thermal calculation method has been written in MATLAB environment. MATLAB (MATrix LABoratory) is a numerical computational platform with many paradigms and a matrix-based

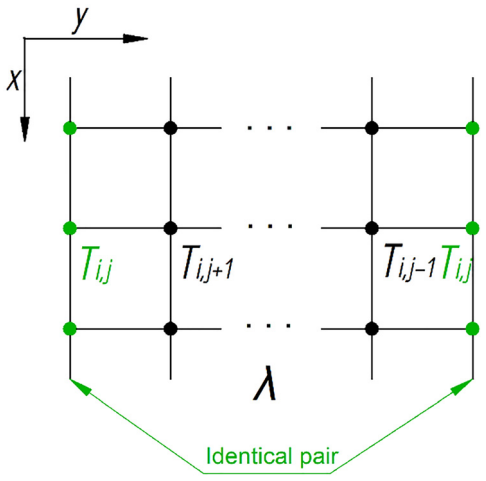

Fig. 9. Identical boundary nodes in FDM mesh (own source)

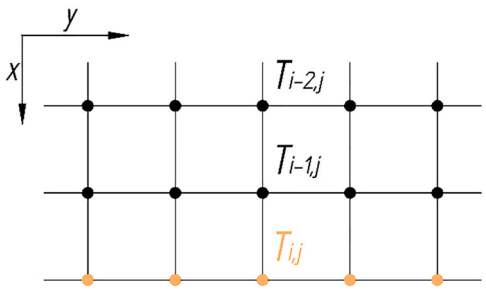

Fig. 10. Perfectly insulated boundary nodes in FDM mesh (own source)

software package launched by MathWorks to express computational mathematics. MATLAB platform is optimized for solving engineering and scientific problems quickly and easily by matrix operations, visualizing functions and data, execution of algorithms, development of user interfaces, and interacting with programs written in other languages, such as C, C++, C#, Java, Fortran or Python. The built-in graphics and add-on toolboxes make it easy to display and gain insights from the numerical results [11].

The script of the developed 2-dimensional thermal calculation model does not need any special skills of damper experts, CFD engineers or material scientists to use. The model requires geometrical data, operational boundary conditions and material properties of the investigated visco-damper product and calculates the temperature field for each component in a 2-dimensional simplified damper cross-section by approximating the hidden heat transfer processes among the inertia-ring, silicone oil film, housing and the ambient. Since it is developed to be a visco-damper specific calculation tool, there is no need for importing CAD models or the creation of a damper geometry as the simplified damper geometry will be automatically calculated from the input sizes of the investigating damper geometry. Also meshing and the visualization of the thermal results are fully automated and there is no need for any interaction from the user's side. Because of these reasons, the developed thermal calculation tool provides thermal results in significantly shorter time compared to a CFD job where the generation of geometry and the numerical meshes are the crucial points in terms of time required. The workflow and the calculation methodology of the created MATLAB code is the following:

1. Taking input parameters from the real 3-dimensional damper geometry and initialization
2. Calculating the radial cross-section of the simplified damper geometry (in 2-dimensions)
3. Calculating heat transfer coefficient and heat source
4. Converting the simplified damper geometry into an equivalent damper geometry
5. Creating coefficient matrix $\left[\overline{\overline{A}}\right]$
6. Creating constant-term vector $\left[\overline{C}\right]$
7. Creating solution vector $\left[\overline{T}\right]$ by solving the matrix equation

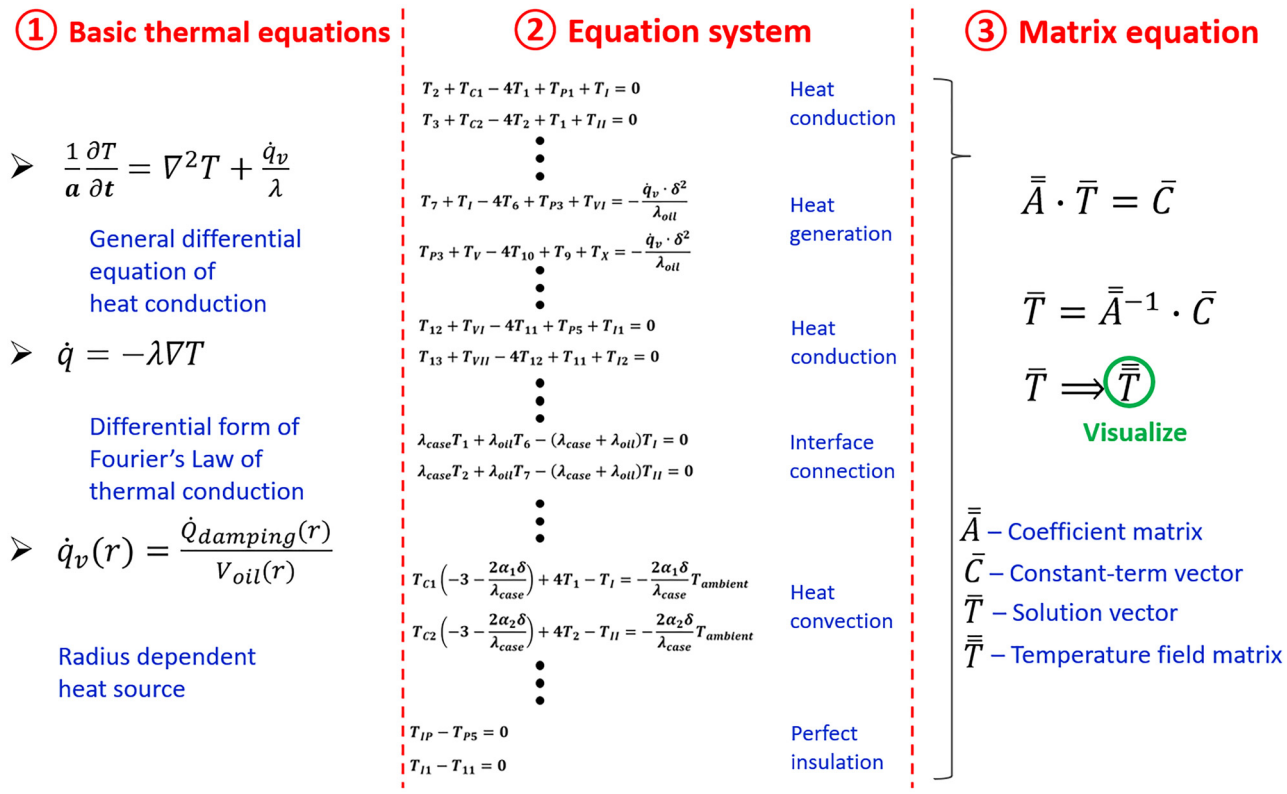

Fig. 11. Setting up the equation system for the numerical solution (own source)

8. Generating the temperature-field matrix $\left[\bar{\bar{T}}\right]$ from the solution vector
9. Plotting the temperature-field matrix on the equivalent damper geometry.

Let us consider a simplified visco-damper geometry with dimensions and material properties presented in Fig. 12. The thickness of silicone oil film and air-gap are specified to be 2 mm, which is the key point by means of the proper mesh

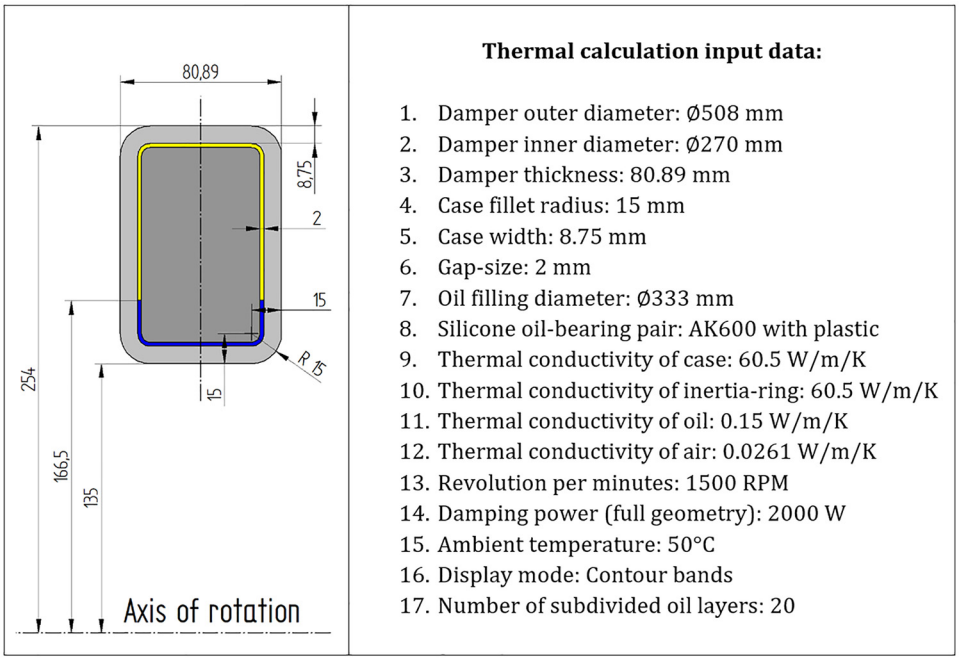

Fig. 12. Damper cross-section (left side) with input data (right side) for example calculation (own source)

and for high accuracy in temperature calculation. As far as finite difference method is concerned, each cell of the applied mesh must be uniform and adjusted to the size of the oil band. Silicone oil must be at least two cell elements thick for heat load definition. At this time, the oil-gap is divided into 20 layers thus the grid spacing is found to be 0.1 mm.

According to the mesh statistics in Table 2, the thermal calculation has been performed on approximately one million nodes. It is considered to be a quite detailed analysis as the total area of the investigated equivalent damper model is 0.0092 m^2 and this tiny face has been divided into almost one million elements.

The calculations have been performed on a desktop PC used for research and development purposes equipped with a quad-core processor. With this computational capacity it took 1 h and 12 min to obtain the results for the finest mesh (20 sublayers of the oil-gap). Computational time is crucial in R&D activities, thus the developed thermal calculation method must be improved with iteration or approximation-based calculation technique, instead of solving directly the matrix equation, in the future in order to save more time and capacity.

2.4.1. Mesh sensitivity analysis. Mesh sensitivity analysis has been performed in a selected point of the FDM mesh with the same geometry and boundary conditions presented above to decide the convergence and how the mesh quality influences the numerical result. As the mesh is getting finer and the calculation process provides the same results, the applied calculation technique is considered mesh-independent and reliable for engineering application. During analysis the grid spacing has been changed from 1 to 0.1 mm by increasing the number of mesh layers in the oil domain (and in the whole model uniformly) from 2 to 20. The temperature results have been recorded and a Weibull-distribution curve has been fitted onto the temperature data as shown in Fig. 13. The Weibull profile converges to a target value (asymptotic limit) which can be approximated by finer mesh and more calculations.

Table 2. Mesh statistics of the FDM example calculation (own source)

Number of nodes in case	272,223
Number of nodes in oil-gap	44,226
Number of nodes in air-gap	21,483
Number of nodes in inertia-ring	588,252
Total number of nodes	926,184
Total number of elements	922,760

It turned out from the mesh sensitivity analysis, that acceptable results will be obtained if the number of mesh layers in the oil domain is selected to be at least 10 or higher. In this case, the deviation from the target value remains under 5% according to Fig. 13. The highest mesh fineness that is still worth applying is found to be 20 mesh layers in the oil domain. Above this fineness, the calculation time and required computing capacity increase significantly but the deviation to the target value does not reduce to a considerable extent. Because of this fact, 20 mesh layers have been applied in the following calculations and the developed finite difference based thermal calculation method is expected to provide converged results.

3. VERIFICATION OF THE DEVELOPED THERMAL CALCULATION METHOD

Carrying out thermal measurements on a working visco-damper under operational condition is a challenging and dangerous task. On the one hand, only the outer surface of the device can provide temperature data. Any device, sensor with geometrical extension and material properties for temperature measurement in the system, especially in the silicon oil, can change the local physical processes as dynamics and heat transfer and so the temperature too. Silicone oil sample cannot be taken while the damper is in operation. Additionally, performing oil degradation tests on working damper attached to a piston engine can take significantly long time till the first damage sign of the oil arises. Moreover, generating torsional oscillations in an operating engine can create very dangerous and unpredictable situations. Since significant amount of kinetic energy is stored in the rotating masses, the test bench and its adjacent region can be heavily destroyed if this amount

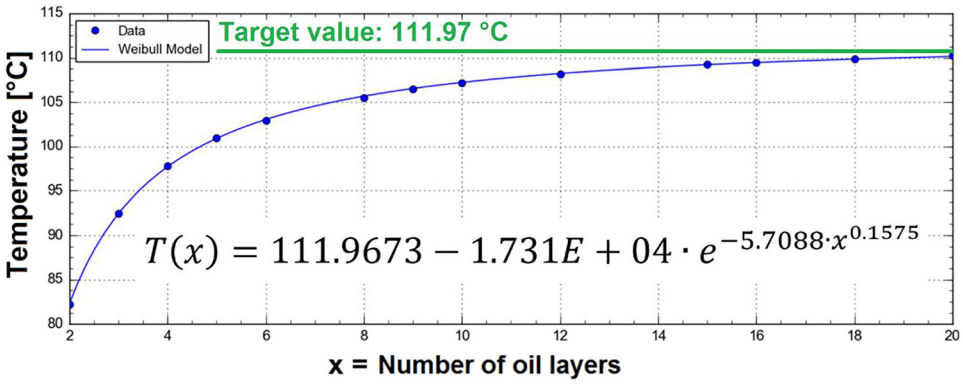

Fig. 13. Weibull distribution curve of the mesh sensitivity analysis (own source)

of energy is released due to a controlling failure or to the loss of control over the rotating system. Because of the collected reasons above, the accuracy of the newly developed finite difference based damper thermal calculation method (FDM) has been tested in a 3-dimensional – 2-dimensional two-step verification process with help of finite element (FEM) and finite volume (FVM) techniques in ANSYS environment.

3.1. Steady-state thermal and CFX submodules in ANSYS

A general-purpose program called ANSYS is used by engineers and researchers worldwide to model interactions across all branches of physics including structural, vibration, fluid dynamics, heat transport, and electromagnetic. In order to analyze in a virtual environment before producing prototypes, it is possible to mimic tests or working situations with ANSYS, by utilizing a range of contact algorithms, time-based loading features, and nonlinear material models [12].

ANSYS Steady-State Thermal submodule (in Mechanical module) has been used for FEM based verification, where the investigated geometry is divided into 1-dimensional and 2-dimensional elements and the Fourier's Law of heat conduction is applied onto them to determine the impact of constant thermal loads on a system or component with determination of temperatures, thermal gradients, heat flow rates, and heat fluxes which do not vary over time. Apart from visco-dampers, FEM is an effective tool for the simulation of other machine elements connected to the internal combustion engines, e.g. sealing [13] or turbocharger bearing housing [14].

ANSYS CFX submodule has been selected for FVM based verification, where the investigated 3-dimensional solid domains are discretized into a collection of control volumes known as cells. The applied energy equations, which form a system of nonlinear partial differential equation, are discretized into a system of algebraic equations. These equations are then solved numerically on the mentioned set of control volumes to render the solution field.

3.2. Selected geometries and operational conditions

Three different damper geometries (see Fig. 14, where Geometry 2 is used for a presentation) have been defined for verification and each geometry has been tested under three different fictitious operational conditions (according to Table 3, with the presented calculation highlighted). These geometries and the considered conditions are not present in the real operations, the goal is to cover the maximal range in the resulting temperature fields including extreme, out-of-order circumstances also. 3-dimensional geometries for FVM calculation (see Fig. 15) with a segment angle of 10° and 2-dimensional geometries for FEM calculation have been created with the same damper dimensions and boundary conditions for each FVM-FEM pair. The heat transfer coefficient on the outer side of the case and heat generation in the oil-gap have been determined as the function of radius for both analyses by applying Eq. (12) and Eq. (19).

3.3. Thermal calculation results

In order to acquire a clear picture about the accuracy of the applied numerical methods, nodal temperature comparison

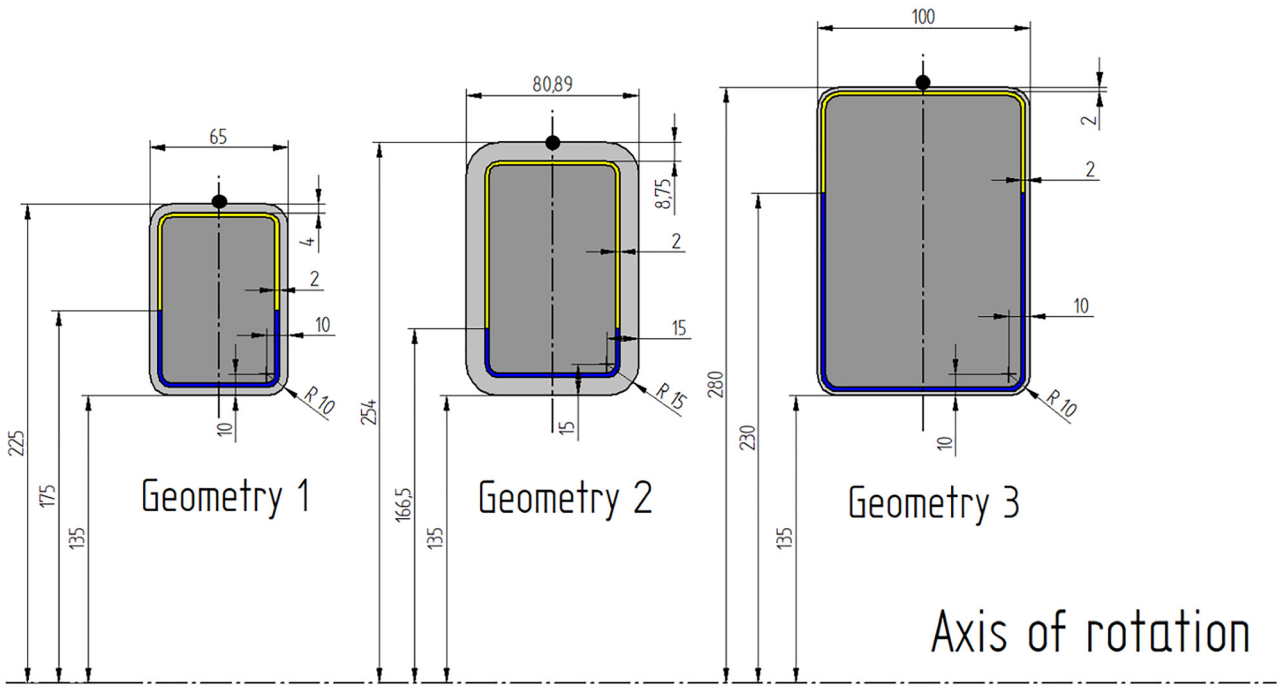

Fig. 14. Different damper geometries for verification (own source)

Table 3. Operational conditions for verification (own source)

Operational condition	Light	Normal	Heavy
Dissipated power [W]	1,000	2,000	4,000
Rotational speed [RPM]	800	1,500	3,000
Ambient temperature [°C]	25	50	80
Silicone oil – bearing pair	AK600 + PA	AK600 + PA	AK600 + PA

due to the fact that three different numerical methods have been applied for the same thermal problem.

The monitored temperature results have been compared for each geometry separately in Fig. 19, Figs 20 and 21. Red colour refers to MATLAB FDM results, while blue colour belongs to ANSYS FVM data and green colour means ANSYS FEM values. Dashed line has been selected for values coming from "Light" (L) operational condition, continuous

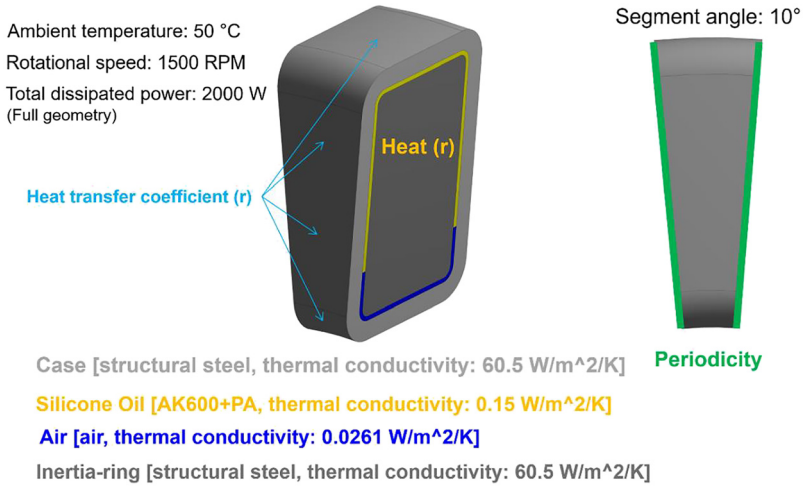

Fig. 15. FVM geometry and boundary conditions of the verification model (own source)

has been performed in pre-defined monitoring points along the damper gap-midline (according to Fig. 16), for each test case with the three applied numerical methods.

Numerical results have been compared to each other in three pairs as shown in Figs 17 and 18. Temperature scales are set to global minimum and global maximum to use them as common scale for the comparison. The black arrows in Fig. 17 show the position of the nodes which belong together. The temperature field and contour distribution show similarities in each comparison with minor differences

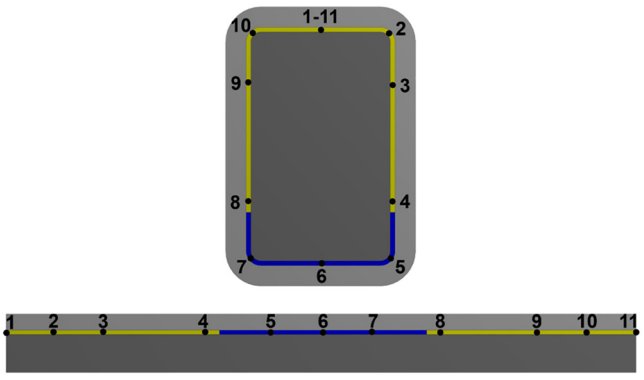

Fig. 16. Monitoring points along the damper gap-midline (own source)

line refers to the "Normal" (N) conditions and values taken from "Heavy" (H) conditions are presented by dotted line

In terms of FDM – FEM comparison, the highest relative deviation is 6.10% at Geometry 2 "Light" operation in point 6. The average relative deviation in this method-pair comparison is 2.18%. As far as FDM – FVM comparison is concerned, the highest relative deviation is 9.33% at Geometry 3 "Light" operation in point 4 and point 8. The average relative deviation in this method-pair comparison is 3.45%. Comparing FVM results to FEM results, the highest relative deviation is 7.68% at Geometry 3 "Light" operation in point 4 and point 8. The average relative deviation in this method-pair comparison is 4.21%.

As far as the surface temperature of the housing is concerned, the highest values, gained by FDM, are calculated for Geometry 1. In the case of "Light" operation, the highest surface temperature is found to be 92.3 °C; while in the case of "Normal" operation this value is 138.79 °C and in the case of "Heavy" loading condition 192.85 °C is calculated. Homik et al. in their work [5] performed surface temperature measurements via laser pyrometer and claimed an operational surface temperature range of 80–125 °C for visco-dampers filled with silicone oils in different viscosities. However, the dissipated power, the rotational speed and the size of the test damper in their measurements are not known, the magnitude of surface temperature results in the current paper shows a good agreement with the measured temperature range presented in [5].

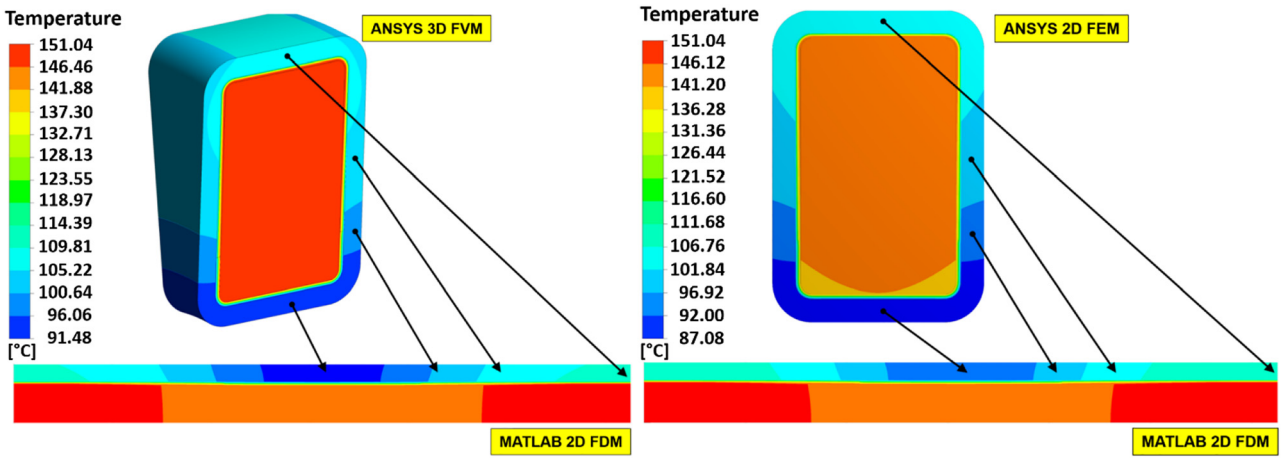

Fig. 17. Comparison of FVM – FDM results (left) and FEM – FDM results (right) in example calculation (own source)

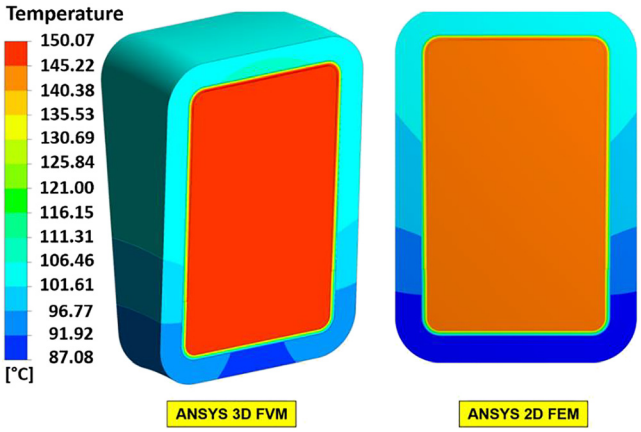

Fig. 18. Comparison of FVM – FEM results in example calculation (own source)

The developed thermal calculation method provides not only converged but highly accurate results with acceptable relative deviations (less than 10%), thus the created MATLAB code is suitable for engineering calculations for visco-damper applications. The advantages, applicability conditions and additional features of the developed method are collected in Table 4.

4. UPDATING THE IWAMOTO-EQUATION

4.1. Original Iwamoto-equation

To perform a preliminary thermal study of visco-dampers by determining the outer surface temperature of the damper housing (calculated in the Iwamoto point, marked by black dot in Fig. 14) under operation, a half-empirical analytical expression [15] created by S. Iwamoto is available in the literature. This expression is described by Eq. (24).

$$\dot{Q} = 112.1 \cdot a \cdot \omega^{0.8} \cdot A^{1.3} \cdot (T_s - T_{amb}) \cdot e^{-0.00176 \cdot T_s} \qquad (24)$$

Where $\dot{Q}$ is the total damping power [W], a is the Iwamoto coefficient, ω is the angular velocity of the housing [rad s^{-1}], A is the outer surface of the housing [m^2], T_s is the surface temperature in the Iwamoto point [°C] and T_{amb} is the ambient temperature [°C].

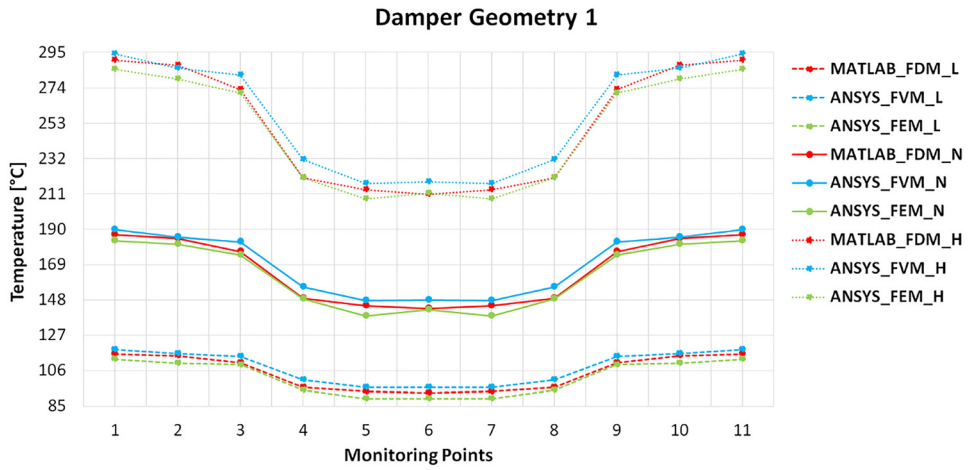

Fig. 19. Temperature values along the gap-midline in Geometry 1 (own source)

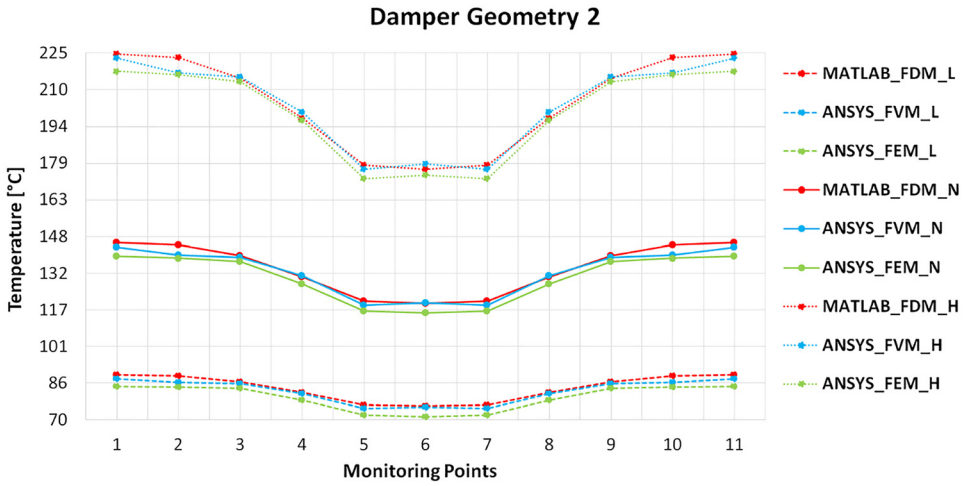

Fig. 20. Temperature values along the gap-midline in Geometry 2 (own source)

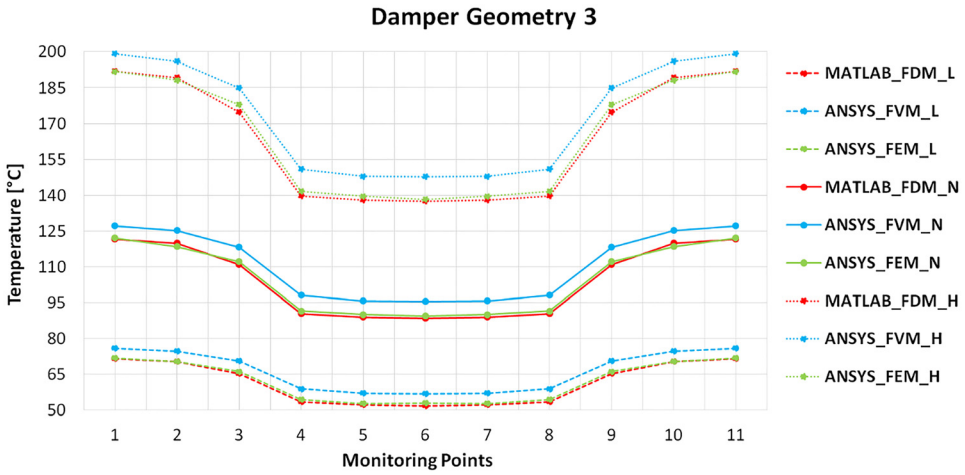

Fig. 21. Temperature values along the gap-midline in Geometry 3 (own source)

The above presented Iwamoto-equation is considered a transcendental equation [16] as there is no closed-form solution for expressing variable T_s. After substituting the known values (damping power, Iwamoto-coefficient, angular velocity, outer surface and ambient temperature), a root-finding technique (e.g. Newton-Raphson method) must be applied to obtain the unknown T_s value. The above presented equation is valid only in a narrow size range ($D_0/D_i = 1.7 \div 2.2$, where D_0 is the outer diameter of the damper's housing and D_i is the inner diameter of the inertia-ring), thus, the verification geometries (presented in Fig. 14) have been selected such a way that their sizes ($D_0/D_i = 1.67 \div 2.07$) well cover and present the validity range of the original Iwamoto-equation. The equation has been tested on each verification geometries under each operational condition and found to provide different results than the numerical investigations (presented in Table 5, where T_{s_FVM} means the surface temperature in the Iwamoto point calculated by 3-dimensional FVM simulation). The highest relative deviation is 33.93% occurred on Geometry 1 under light operating condition and the average of the relative deviations is 23.02%, that is not acceptable for engineering applications. Because of this fact, the equation has to be updated by nonlinear regression and parameter identification with help of the 3-dimensional finite volume method based numerical results.

4.2. Updated Iwamoto-equation

Each constant of the original Iwamoto-equation has been selected for optimizable parameter ($p_1 = 112.1$; $p_2 = 0.8$; $p_3 = 1.3$; $p_4 = -0.00176$) and T_{s_FVM} is selected for the target T_s value in each geometry and operating condition case. The optimization task is simplified into an extremum search where the optimizable cost function can be written in Eq. (20). The local minimum of the cost-function (see Eq. (25)) has been found by MATLAB with help of the built-in "fminsearch" function.

Table 4. Advantages, applicability conditions and additional features of the developed 2-dimensional thermal calculation method (own source)

Aspects	Items
Advantages	• Fast, accurate, and best solution with utilizing all advantages of the FDM including the option for parallelization. • Goal-oriented and cost-effective procedure. • There is no need for knowledge in the field of simulation engineering. • User-friendly, easy to use, and automatic. • Fast preparation: there is no need for detailed pre- and postprocessing. • Best approach for concept analyses and checking preliminary designs.
Applicability conditions	• Only used for thermal calculations in steady-state thermal conditions. • Only used for 2-dimensional damper geometry (cross-section) without cooling fins. • Only used for simplified damper geometry (uniform gap size, rounding, symmetry). • The oil-gap has to be divided into at least 2 layers for heat generation definition. • Acceptable results will be gained with oil-gap divided into 10–15 layers.
Additional features	• Silicone oil and air-gap are treated as solid domains. • Heat radiation is negligible. • The effect of cooling fins mounted on the housing is out of focus. • The heating effect of engine is out of focus. • The generated heat and convected heat are the function of radius. • Calculation is performed for a unit time in steady state condition.

$$\sum_{i=1}^{9} |T_s - T_{s\_FVM}| \Rightarrow \begin{matrix} p_1 \\ p_2 \\ p_3 \\ p_4 \end{matrix} \; min \tag{25}$$

As a result, the updated Iwamoto-equation with 10-digit precision is expressed by Eq. (26) and the improved accuracy of the updated equation is presented in Table 6.

$$\dot{Q} = 109.8594625502 \cdot a \cdot \omega^{0.7553085697} \cdot A^{1.3707718782} \cdot (T_s - T_{amb}) \cdot e^{-0.0017649324 \cdot T_s} \tag{26}$$

The highest relative deviation is reduced to 9.32% occurring on Geometry 2 under heavy operating condition and the average of the relative deviations is reduced to 5.44%, that is acceptable for engineering applications.

5. CONCLUSIONS

In this article a reliable, fast and accurate finite difference based numerical method has been developed for 2-dimensional steady state thermal calculations in a given visco-damper radial cross-section (by applying geometry equivalence theory and visco-damper-specific heat transfer calculations). The heat dissipation due to the damping mechanism is considered as nodal heat source in the function of radius.

The accuracy of the developed thermal calculation method has been tested by finite element and finite volume based advanced engineering software in ANSYS environment. The highest relative deviation in verification points remains under 10%. As the developed MATLAB code is considered to be the first step of a design tool development, the calculation method is acceptable under the investigated conditions. As a result of the parameter identification of updated Iwamoto-equation, the accuracy of the original equation is improved from 33.93% highest relative deviation to 9.32% while the average of the relative deviations is reduced from 23.02% to 5.44%.

As the next steps of this work, the calculation time must be reduced by applying an advanced matrix solver; the

Table 5. Accuracy of the original Iwamoto-equation checked by FVM results (own source)

	Geometry 1			Geometry 2			Geometry 3		
Operating condition	Light	Normal	Heavy	Light	Normal	Heavy	Light	Normal	Heavy
$\lvert T_s - T_{s\_FVM} \rvert$	31.74 °C	41.91 °C	53.31 °C	14.31 °C	17.97 °C	21.64 °C	15.04 °C	20.74 °C	26.7 °C
Relative deviation to T_{s_FVM}	33.93%	30.08%	27.79%	20.71%	16.93%	14.56%	23.83%	20.69%	18.69%

Table 6. Accuracy of the updated Iwamoto-equation checked by FVM results (own source)

	Geometry 1			Geometry 2			Geometry 3		
Operating condition	Light	Normal	Heavy	Light	Normal	Heavy	Light	Normal	Heavy
$\lvert T_s - T_{s\_FVM} \rvert$	8.42 °C	8.18 °C	5.97 °C	3.67 °C	7.71 °C	13.84 °C	2.62 °C	3.14 °C	2.62 °C
Relative deviation to T_{s_FVM}	9%	5.87%	3.11%	5.32%	7.26%	9.32%	4.15%	3.13%	1.83%

running time of the code must be decreased by execution in parallel computing (e.g.: executing on video card); temperature dependent material properties must be considered instead of constants; oil lifetime calculation models must be integrated into the calculation method (based on accelerated oil degradation tests with equivalent degradation theory and proper cumulative damage model for oil degradation); thermal and rheological measurements must be performed for validation purpose.

ACKNOWLEDGEMENTS

The presented research is supported by the Hungarian Automotive Higher Education Foundation. This work was supported by Hungarian national EFOP-3.6.1-16-2016-00014 project titled by "Investigation and development of the disruptive technologies for e-mobility and their integration into the engineering education". Special thanks to Gábor Rácz and the Engineering Calculations Team of Knorr-Bremse R&D Center Budapest for their technical support in CFD.

REFERENCES

[1] K. R. Mobley, *Vibration Fundamentals*. 1st ed. Butterworth-Heinemann, 1999, ISBN: 9780750671507.

[2] Geislinger gmbH, "*VDamp®*", Product catalogue. [Online]. Available: https://www.geislinger.com/cms_images/products/Vdamp_1.6.pdf. Accessed: Jan. 12, 2023.

[3] M. Wang, R. Zhou, and X. Xu, "The engine silicone-oil damper matching calculation method based on the heat balance", *Res. J. Appl. Sci. Eng. Technol.*, vol. 4, no. 16, pp. 2773–7, 2012.

[4] A. Forberger, "Calculating the dissipation in fluid dampers with non-newtonianfluid models", *Mech. Res. Commun.*, vol. 67, pp. 18–23, 2015.

[5] W. Homik, A. Mazurkow, and P. Woś, "Application of a thermo-hydrodynamic model of a viscous torsional vibration damper to determining its operating temperature in a steady state", *Materials*, vol. 14, no. 18, 5234, 2021.

[6] COMSOL, "*The Finite Element Method (FEM)*", Website, 2017. [Online]. Available: https://www.comsol.com/multiphysics/finite-element-method. Accessed: Jan. 12, 2023.

[7] A. Cerovský, A. Dulce, A. Ferreira, "*Application of the Finite Difference Method and the Finite Element Method to Solve a Thermal Problem*", Department of Mechanical Engineering, Integrated Masters in Mechanical Engineering, University Porto, Porto, Portugal, 2014. [Online]. Available: https://www.estudomec.info/files/SPT_Analise_Termica_MEF_MDF.pdf. Accessed: Jan. 12, 2023.

[8] Y. A. Çengel, "*Heat Transfer: A Practical Approach*", 2nd ed. Mcgraw-Hill (Tx), 2002, ISBN: 9780072458930.

[9] M. Amiri and M. M. Khonsari, "On the thermodynamics of friction and wear—A review", *Entropy*, vol. 12, no. 5, pp. 1021–49, 2010.

[10] M. Banjac, A. Vencl, and S. Otović, "Friction and wear processes – thermodynamic approach", *Tribol. Ind.*, vol. 36, no. 4, pp. 341–7, 2014.

[11] CIMSS, "What is MATLAB?", Website, 2023. [Online]. Available: https://cimss.ssec.wisc.edu/wxwise/class/aos340/spr00/whatismatlab.htm. Accessed: Jan. 12, 2023.

[12] DesignTech CAD Academy, "Introduction to Ansys", Website, 2023. [Online]. Available: https://www.designtechcadacademy.com/knowledge-base/ansys-software. Accessed: Jan. 12, 2023.

[13] J. Grün, S. Feldmeth, and F. Bauer, "The sealing mechanism of radial lip seals: a numerical study of the tangential distortion of the sealing edge", *Tribol. Mater.*, vol. 1, no. 1, pp. 1–10, 2022.

[14] E. Zadorozhnaya, V. Hudyakov, and S. Sibiryakov: "Simulation of heat transfer in a turbocharger bearing housing", *Tribol. Mater.*, vol. 1, no. 2, pp. 42–54, 2022.

[15] K. E. Hafner and H. Maass, "Torsionsschwingungen in der Verbrennungskraftmaschine" in *Die Verbrennungskraftmaschine* Neue Folg, Band 4, 1st ed. Wien-New York: Springer, 1985, ISBN: 9783211817933.

[16] J. P. Boyd, "*Solving Transcendental Equations: the Chebyshev Polynomial Proxy and Other Numerical Rootfinders, Perturbation Series, and Oracles*", Illustrated edition, Society for Industrial and Applied Mathematics, 2014, ISBN: 9781611973518.